AD-A182 496 EXPERIMENTAL SURVEY AND HEAT FLUX PREDICTION FOR THERMAL/CHEMICAL MISMATCHES(U) AIR COMMAND AND STAFF COLL MAXWELL AFB AL J K HODGE APR 87 ACSC-87-1205 1/1

UNCLASSIFIED F/G 20/13 NL

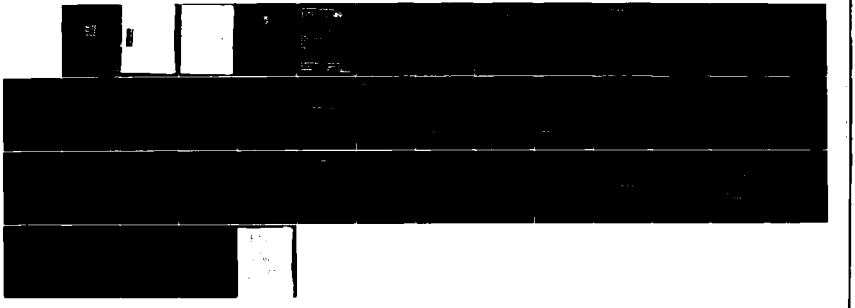

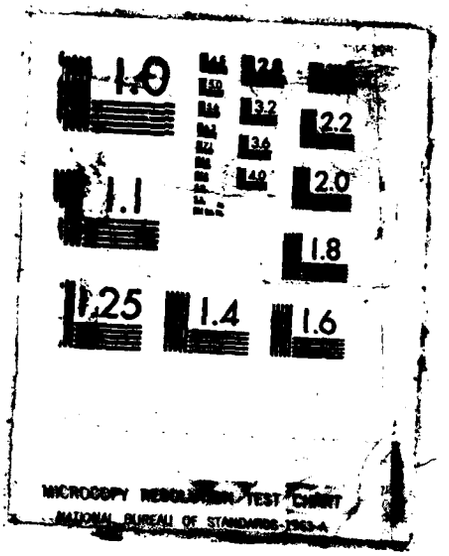
1.0
1.1
1.25
1.4
1.6
1.8
2.0
2.2
2.4
2.5
3.2
3.6
4.0
MICROCOPY RESOLUTION TEST CHART
NATIONAL BUREAU OF STANDARDS-1963-A

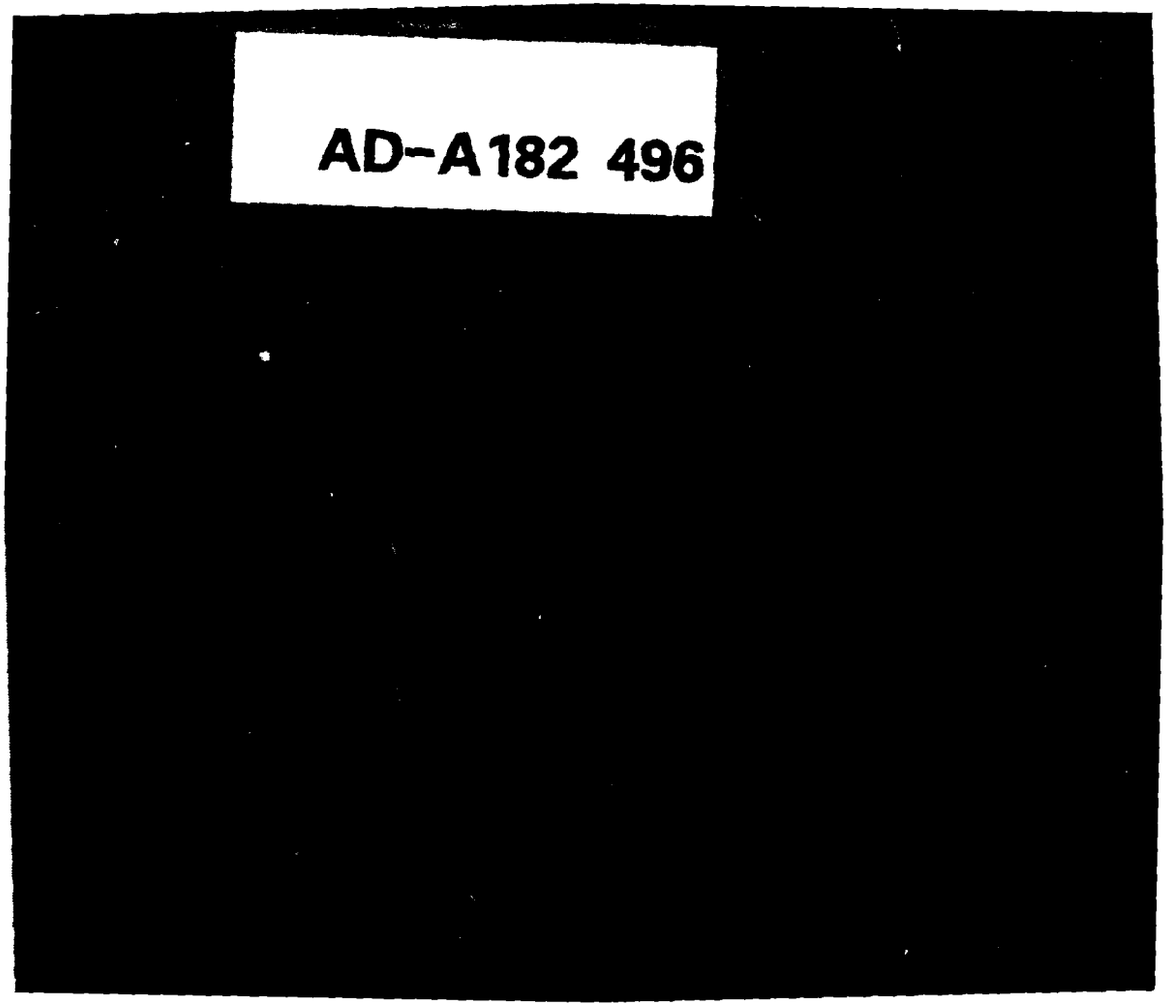
AD-A182 496

REPORT NUMBER 87-1205

TITLE EXPERIMENTAL SURVEY AND HEAT FLUX PREDICTION FOR THERMAL/CHEMICAL MISMATCHES

AUTHOR(S) MAJOR JAMES K. HODGE, USAF

FACULTY ADVISOR MAJOR MICHAEL A. WHITE, USAF

SPONSOR JOURNAL OF THERMOPHYSICS & HEAT TRANSFER

Submitted to the faculty in partial fulfillment of requirements for graduation.

AIR COMMAND AND STAFF COLLEGE
AIR UNIVERSITY
MAXWELL AFB, AL 36112

UNCLASSIFIED
SECURITY CLASSIFICATION OF THIS PAGE

A182496

REPORT DOCUMENTATION PAGE

1a. REPORT SECURITY CLASSIFICATION UNCLASSIFIED	1b. RESTRICTIVE MARKINGS
2a. SECURITY CLASSIFICATION AUTHORITY	3. DISTRIBUTION/AVAILABILITY OF REPORT STATEMENT "A" Approved for public release Distribution is unlimited.
2b. DECLASSIFICATION/DOWNGRADING SCHEDULE	
4. PERFORMING ORGANIZATION REPORT NUMBER(S) 87-1205	5. MONITORING ORGANIZATION REPORT NUMBER(S)
6a. NAME OF PERFORMING ORGANIZATION ACSC/EDCC — 6b. OFFICE SYMBOL (If applicable)	7a. NAME OF MONITORING ORGANIZATION
6c. ADDRESS (City, State and ZIP Code) Maxwell AFB, AL 36112-5542	7b. ADDRESS (City, State and ZIP Code)
8a. NAME OF FUNDING/SPONSORING ORGANIZATION — 8b. OFFICE SYMBOL (If applicable)	9. PROCUREMENT INSTRUMENT IDENTIFICATION NUMBER
8c. ADDRESS (City, State and ZIP Code)	10. SOURCE OF FUNDING NOS. PROGRAM ELEMENT NO. — PROJECT NO. — TASK NO. — WORK UNIT NO.
11. TITLE (Include Security Classification) EXPERIMENTAL SURVEY AND HEAT	
12. PERSONAL AUTHOR(S) Hodge, James K., Major, USAF	
13a. TYPE OF REPORT — 13b. TIME COVERED FROM ____ TO ____ — 14. DATE OF REPORT (Yr., Mo., Day) 1987 April — 15. PAGE COUNT 42	
16. SUPPLEMENTARY NOTATION ITEM 11: FLUX PREDICTION FOR THERMAL/CHEMICAL MISMATCHES	
17. COSATI CODES FIELD — GROUP — SUB. GR	18. SUBJECT TERMS (Continue on reverse if necessary and identify by block number)

19. ABSTRACT (Continue on reverse if necessary and identify by block number)

Material interfaces are common in heat flux instrumentation and in modern thermal protection systems. Interfaces cause mismatches which can significantly affect convective heat flux. A literature survey on chemical and thermal mismatches with emphasis on experimental data is presented. Data indicate transient variations in heat transfer coefficient. Unsteady boundary layer equations are solved computationally using upwind differences and parabolic grid generation. Results are compared with data, and other computational and analytical solutions, to investigate solution accuracy across a mismatch. By coupling wall conditions, transient variations in heat transfer coefficient at a given deflection angle are computed on Space Shuttle Orbiter materials near an interface during unsteady pitch manuevers. KEYWORDS: FLUX PREDICTION

20. DISTRIBUTION/AVAILABILITY OF ABSTRACT UNCLASSIFIED/UNLIMITED ☐ SAME AS RPT ☒ DTIC USERS ☐	21. ABSTRACT SECURITY CLASSIFICATION UNCLASSIFIED
22a. NAME OF RESPONSIBLE INDIVIDUAL ACSC/EDCC Maxwell AFB AL 36112-5542	22b. TELEPHONE NUMBER (Include Area Code) (205)293-2483 — 22c. OFFICE SYMBOL

DD FORM 1473, 83 APR — EDITION OF 1 JAN 73 IS OBSOLETE.

UNCLASSIFIED
SECURITY CLASSIFICATION OF THIS PAGE

PREFACE

Thermal protection systems are of critical importance to the survival of any aerospace vehicle that flys at high speeds, especially at hypersonic and reentry speeds. For unmanned vehicles, such as ballistic missile warheads or interplanetary probe vehicles must have reasonable safety margins to survive and effectively perform their mission. For manned vehicles, such as the Space Shuttle or the newly proposed National Aerospace Plane (NASP), safety margins become even more important. Therefore, accurate aerothermodynamic heat transfer predictions and measurements are needed to insure margins, and so that the weight of thermal protection systems can be minimized.

Numerous materials which are very light are being used in modern thermal protection systems, and cause numerous material interfaces. These interfaces can cause significant changes in surface heat transfer predictions and measurements, which have often been ignored. Measurements have often been misinterpreted, and vehicles usually over-designed. Unfortunately, this has occurred on numerous unmanned and manned vehicles, and much of the data can not be published.

Some published data has been discovered during a literature survey, which can be used to validate new computational methods to accurately predict heat transfer near interfaces. The new computational method presented in this research originated with the author, but implementation has been accomplished with the help of several students at the Air Force Institute of Technology. First Lieutenant Karen Lange started the computer program used, and subsequently Captain Alice Chen extended the program. The author further extended, corrected, and applied the program to obtain results presented in this research.

Subject to clearance, this manuscript will be submitted to the Journal of Thermophysics and Heat Transfer which is published by the American Institute of Aeronautics and Astronautics (AIAA) for consideration.

ABOUT THE AUTHOR

Major James K. Hodge received Bachelor of Science and Master of Science degrees in Aerospace Engineering from Mississippi State University in 1970 and 1972 respectively. He was also commissioned through the ROTC program in 1972. After a two year educational delay, he received the Doctor of Philosophy Degree in Engineering. His first assignment was to the Air Force Flight Dynamics Laboratory at Wright-Patterson Air Force Base as a computational aerodynamicist. His next assignment was in 1977 to the 6510th Test Wing, Space Shuttle Office, at Edwards AFB as an aerothermodynamicist and test engineer where he participated in the Orbital Flight Test Program for the Space Shuttle. He was a member of the Thermal Protection System inspection team after the first five flights. His third assignment was in 1982 to the Air Force Institute of Technology, Aeronautics and Astronautics Department, at Wright-Patterson as an Associate Professor.

Major Hodge has specialized in three areas including computational aerodynamics, aerthermodynamics, and systems identification theory. In these areas, he has taught six undergraduate and nine graduate courses, and advised sixteen master's theses and one dissertation. Research by these students and by Major Hodge supported numerous Air Force and other government agencies. Because of this research, he has given over fifteen public presentations, and published twenty-four papers and articles. The following are representative samples.

Hodge, J. K. and Stone, A. L., "Numerical Solution for Hypersonic Near Stall in Optimized Boundary-Fitted Curvilinear Coordinates. AIAA Paper 78-284 and AIAA Journal, Vol. 17, 1979, pp. 456-464.

Hodge, J. K., Audley, D. R., and Phillips, P. W., "Aerothermodynamic Flight Envelope Expansion for a Manned Lifting Reentry Vehicle (Space Shuttle)," AGARD CP-339, Cesme, Turkey, 1982.

Hodge, J. K. and Audley, D. R., "Aerothermodynamic Parameter Estimation from Space Shuttle Thermocouple Data During Transient Flight Test Maneuvers," AIAA Paper 83-0482 and Journal of Spacecraft and Rockets, Vol. 23, 1986, pp. 453-460.

TABLE OF CONTENTS

LIST OF ILLUSTRATIONS

EXPERIMENTAL SURVEY AND HEAT FLUX PREDICTION FOR THERMAL/CHEMICAL MISMATCHES

Major James K. Hodge*
Air Command and Staff College
Air University
Maxwell Air Force Base, Alabama

ABSTRACT

Material interfaces are common in heat flux instrumentation and in modern thermal protection systems. Interfaces cause mismatches which can significantly affect convective heat flux. A literature survey on chemical and thermal mismatches with emphasis on experimental data is presented. Data indicate transient variations in heat transfer coefficient. Unsteady boundary layer equations are solved computationally using upwind differences and parabolic grid generation. Results are compared with data, and other computational and analytical solutions, to investigate solution accuracy across a mismatch. By coupling wall conditions, transient variations in heat transfer coefficient at a given deflection angle are computed on Space Shuttle Orbiter materials near an interface during unsteady pitch manuevers.

NOMENCLATURE

c_p	Specific heat
C_f	Skin friction coefficient
h	Heat transfer coefficient; $q/(T_{aw} - T_w)$
H	Nondimensional total enthalpy
L	Reference Length
M	Mach number
p	Nondimensional pressure

* AIAA Member. Former Associate Professor of Aeronautics & Astronautics at Air Force Institute of Technology.

Pr	Prandtl number
q	Heating rate
R	Nondimensional surface radius
Re	Reynold's number
St^*	Stanton number; $q/(T_\infty - T_w)/c_p\rho u_\infty$
t	Nondimensional time
T	Temperature
u	Nondimensional tangential/axial velocity
v	Nondimensional normal velocity
V	Transformed normal velocity
x	Nondimensional tangential/axial coordinate
y	Nondimensional normal coordinate
Y	Transformed normal coordinate

Greek

ξ, η	Transformed coordinates
μ	Nondimensionalized viscosity
ρ	Nondimensionalized density
δ	Deflection angle

Subscripts

$(\cdot)$	Denotes differentiation
aw	Denotes adiabatic wall
j	Denotes normal grid point index
o	Denotes stagnation condition
T	Denotes turbulent quantity
w	Denotes wall quantity
∞	Denotes freestream quantity

Superscript

m	Two-dimensional/axisymmetric indicator

INTRODUCTION

Modern thermal protection systems for reentry vehicles, such as Space Shuttle, usually have different materials which interface at numerous locations. Heat flux instrumentation imbedded in these vehicles and in models used in ground tests have similar interfaces. These interfaces cause mismatches which may significantly affect wall temperatures and convective heat flux.

Several types of mismatches can occur at material interfaces, as illustrated by the following examples. First, a physical mismatch can be caused by a forward or backward facing step at the surface of an interface. A step causes flow disturbances which cause local changes in convective heat flux. Second, a radiative mismatch can be caused by different surface emissivities. Thus, heat radiated from each side of the interface would be different, and could result in a wall temperature discontinuity referred to as a thermal mismatch. A thermal mismatch can also be caused by materials with different thermal properties, cause different wall temperature responses, and result in a discontinuity in the wall temperature distribution if conductivities are very low. A fourth type of mismatch, a chemical mismatch, can be caused by coatings with different catalytic efficiencies for the recombination of dissociated nitrogen and oxygen (a chemical nonequilibrium effect). This discontinuity in surface catalysis can cause a discontinuity in recombination energies which contribute to the heat flux. Of these mismatches, the thermal and chemical mismatch have often been neglected perhaps because they were not significant, and perhaps because of diffi-

culty in realistically accounting for them.

The thermal and chemical mismatch are difficult to account for because of dependence upon local and upstream wall conditions. For example, consider an interface with a hot-noncatalytic wall upstream and with a cold-fully catalytic wall downstream. During reentry, part of the kinetic energy of the freestream air is converted and stored, thermally by increasing the gas temperature and chemically by dissociating the gas. Since less energy is transported to the upstream wall (heat flux) than for a cold-fully catalytic wall, additional energy is convected downstream across the interface. Downstream of the interface, there is a jump in heat flux because the wall is cold and fully catalytic. The additional energy convected across the interface causes an additional overshoot in heat flux. Thus, the heat flux depends on upstream and local wall conditions, which are usually transient during ground tests and reentries.

Since numerous materials with different properties and varying degrees of catalytic efficiency are being used, a method of evaluating the significance of an interface on the aerothermodynamic design of a vehicle (and heat flux instrumentation) is needed. Experimental flight and ground tests, approximate analytical solutions, and computational solutions are possibilities. Only a few references (which will be presented in the next section) are available on mismatches with one exception; numerous approximate analytical methods are published on a thermal mismatch with a discontinuous step (and will not be presented). A solution for a chemical mismatch with two species is also availa-

ble, but is not extended in general for reacting multi-species with finite recombination rates. Some ground test data are available for a thermal mismatch with a discontinuous step on simple configurations, but ground facilities can not simulate some variations in wall conditions, nor duplicate flight conditions. Computational solutions are becoming widespread, and can be as general as needed, including transient solutions. But, the accuracy of computational solutions is of concern because of the discontinuities at mismatches. However, computational solutions have been successfully applied to available ground and flight data at chemical mismatches to correlate rate coefficients. Unfortunately, no solutions have been computed to explain some transient effects near a mismatch during unsteady pitch manuevers in both ground and flight tests.

Besides evaluating the significance of mismatches, the primary purpose of this article is to present and apply a unique (but simple) computational method to investigate steady and unsteady solution accuracy at mismatches using a combination of the above methods. First, a literature survey is presented which covers available experimental, analytical, and computational investigations of the thermal and chemical mismatch. Next, a computational solution of the unsteady boundary layer equations has been developed using three-point upwind differences and parabolic grid generation. This unique approach minimizes computer resources needed for transient solutions, but uses differencing techniques and arbitrary grids applicable for Navier-Stokes solutions. Next, upwind difference solutions are validated by comparing with

analytical solutions, central difference solutions, and experimental data. Although solutions for a chemical mismatch have been computed, results are not presented since a thermal mismatch is analogous and can be validated easier. Finally, the upwind difference solution is coupled with wall temperatures to predict transient variations in heat transfer distributions during an unsteady pitch manuever with a wedge in a wind tunnel test.

LITERATURE SURVEY

A literature survey was conducted primarily on heat transfer data for chemical and thermal mismatches, but also included some analytical and computational solutions. References for chemical mismatches will be discussed first. Then a comprehensive survey of published experimental data for a thermal mismatch will be presented. Next, details will be given of some data which will be used to compare with computational solutions. Finally, some data which have indicated transient trends in heat transfer coefficient will be discussed.

Chung, Liu, and Mirels predicted the boundary layer profiles and heat flux for a chemical mismatch in a reacting binary mixture.[1] The overshoot in heat transfer at a chemical mismatch was confirmed by their theoretical solution of the boundary layer equations, although catalytic efficiencies for various materials were not well known. Based on their solution, a gage with known catalytic efficiency imbedded in a material of unknown efficiency was proposed to determine catalytic efficiency. The multiple species in air during flight complicates the proposal. If air is approximated as a binary mixture, then their solution can vali-

date computational solutions across a chemical mismatch.

Sheldahl and Winkler confirmed the significance of a chemical mismatch in arc-plasma tests by using various combinations of silicon oxide(SiO) and copper(Cu) coatings on a hemisphere-cylinder.[2] For example, the heating on the cylinder with the Cu coating was more than twice the heating with a SiO coating. The heating significantly quadrupled with a SiO/Cu interface.

Stewart, Rakick, and Lanfranco also confirmed the significance of a chemical mismatch in arc-plasma tests for the Space Shuttle Orbiter's thermal protection system by alternatively using the baseline coating of borosilicate glass, and then a catalytic overcoat of iron-cobalt-chromia-spinal.[3] Again, the heat transfer at locations downstream of a noncatalytic/catalytic interface exceeded heat transfer rates for chemical equilibrium. Recombination rate constants were then adjusted in a computational solution for a reacting boundary layer to match predicted and measured heat transfer ratios. Recombination rate constants were then assumed, and similar overshoots predicted for a flight test experiment where individual tiles on the lower surface of the Orbiter were coated with the same catalytic overcoat.

Shuttle flight results published by Rakick, Stewart, and Lanfranco (and by Scott and Derry) confirmed the overshoot in heat transfer at the chemical mismatch caused by the overcoat.[4,5] Recombination rates had to be adjusted for postflight predictions. However, oxygen and nitrogen recombination rates can not be determined independently since their effects are lumped in flight results. In addition, the chemical mismatch causes a

thermal mismatch which becomes more significant at lower Mach number. Such a combined chemical/thermal mismatch was assumed by Curry, Rochelle, Chao, and Ting for computational predictions at the Orbiter's nose cap/tile interface.[6]

A comprehensive survey of published experimental data for a thermal mismatch provided several references. Data for a thermal mismatch with a step in wall temperature are given by Scesa for incompressible, turbulent flow over a flat plate.[7] A more thorough study for incompressible, turbulent flow over a plate with a step in wall temperature is given by Reynolds, Kays, and Kline.[8] Laminar data for incompressible flow are given by Ede and Saunders for a flat plate in water,[9] but erratic data indicate subsequent transition to turbulent flow. McCroskey published results for laminar supersonic flow over a flat plate with a step in heat flux.[10,11] Praharaj and Foster presented flight data for the Space Shuttle external tank during ascent which show a significant effect on heat flux instrumentation due to a thermal mismatch.[12] Data were corrected by a factor of two, but no correction is available where complex flow interactions are expected. Finally, Durgin published excellent results for both laminar and turbulent supersonic flow over a cone.[13,14] Data from two of these references will be discussed in more detail.

The experimental data for turbulent flow over a flat plate with heating strips was selected to compare with computational solutions.[8] The plate is illustrated in Figure 1. The first four strips were unheated, and the remaining strips were heated to maintain a step in wall temperature. Due to the low freestream

Reynold's number of 2.96×10^6 (0.5×10^6 at the thermal mismatch), a trip wire was used after the second heating strip to transition the flow. Although this data is considered to be for incompressible flow, a freestream Mach number of 0.08 was computed for use in the compressible algorithms.

Wall temperature data on a cone with a thermal mismatch are available for compressible flow at Mach 3.5.[13,14] An illustration of the cone is shown in Figure 2. The copper nose was cooled for a uniform wall temperature of 233°K. The aft part of the cone was made of balsa wood, which approximated an adiabatic wall. Data are given for both laminar and turbulent flows with freestream Reynold's numbers of 2.06 and 7.52×10^6 respectively. Since numerous thermocouples were along the wall of the cone (and uncertainty avoided in determining heat flux), this data was also selected for computational comparisons.

Recent data for a wedge shown in Figure 3 with a thermal mismatch are also used for computational comparisons because of some interesting discrepancies.[15] A steel wedge (17.95 x 38.46 cm) with inserts (15.38 x 15.38 cm) starting at 17.95 cm from the leading edge was pitched between 3° to 14° deflection angles in a Mach 14.24 wind tunnel to simulate Space Shuttle Orbiter flight pitch manuevers. The hypersonic flow was laminar because of low Reynold's number (1.2×10^6). One insert was Flexible-Reusable-Surface-Insulation(FRSI) from the Orbiter's thermal protection system. The heat transfer coefficient to the FRSI was dramatically lower because of the mismatch, but was also lower than predicted. Data reduction problems encountered by Woo indi-

cate that the heat transfer coefficient varied in time at a given deflection angle while the wedge was pitched.[16] Thus, a hysteresis loop occurs when the wedge is pitched down and then up. This loop will be predicted computationally.

In another recent test at Mach 6, a teflon button and coaxial thermocouple gage were imbedded in a blunt-nosed steel plate which was also pitched.[17] A hysteresis loop was indicated by numerous data reduction methods, although results were somewhat different from method to method. Because of experimental difficulties for transient heat flux determination, verification of this transient behavior of the heat transfer coefficient by a theoretical and computational solution is needed.

THEORY (UPWIND DIFFERENCE METHOD)

Since approximate analytical methods can not be extended in general to three-dimensional transient problems, computational methods are becoming more popular. The accuracy of heat transfer predictions are often questioned when computational methods are used especially for discontinuities (such as a mismatch) and for coarse grids. Fine grids can be used, but computational resources may then become very large, especially if the Navier-Stokes equations for the flow are coupled with the heat equation for the wall temperatures. Therefore, a computational method, based on upwind differences, is investigated to solve the unsteady boundary layer equations coupled with various boundary conditions for the wall temperatures. Details of the equations and transformations for arbitrary grids, the upwind difference solution, and boundary conditions are summarized next.

Equations and Transformations

The unsteady boundary layer equations are solved computationally in terms of velocity and total enthalpy. For two-dimensional flow (m=0) or axisymmetric flow (m=1), the governing equations in nondimensional form are given for turbulent flow as

$$R^m\rho_t + (R^m\rho u)_x + (R^m\rho v)_y = 0 \tag{1a}$$

$$(\rho u)_t + (\rho u^2)_x + (\rho uv)_y = -p_x + ([(\mu+\mu_T)u_y]_y)/Re \tag{1b}$$

$$(\rho H)_t + (\rho uH)_x + (\rho vH)_y = p_t + ([(\mu/Pr+\mu_T/Pr_T)H_y + (\mu(Pr-1)/Pr+\mu_T(Pr_T-1)/Pr_T)(\tfrac{1}{2}u^2)_y]_y)/Re \tag{1c}$$

where subscripts denote differentiation. Turbulence closure is accomplished with an eddy viscosity model following Cebeci and Smith.[18] The total enthalpy equation was chosen because of a truncation error criteria. If a Prandtl number of one is assumed, the total enthalpy is a linear function of the tangential velocity for constant properties and isothermal wall conditions. Since gradients of other variables (except density) are small compared to the tangential velocity and enthalpy gradients in the normal direction, optimization of the normal grid distribution for either the velocity or total enthalpy will tend to minimize truncation error. Density gradients are usually not a problem if conservative differencing or a transformation is used.

The compressible boundary layer equations are transformed to eliminate density as a solution variable. Although usually used in a more general form, the transformation given by

$$Y = \int \rho \, dy \tag{2a}$$

$$V = v + Y_t + uY_x \tag{2b}$$

is attributed to Dorodnitsyn by Kim and Chang who solved the

unsteady boundary layer equations using central differences.[19] Some details of the transformation and this approach are available in theses by Lange for laminar flow,[20] by Coffee for an adaptive grid study,[21] and by Chen for turbulent flow.[22]

Contrary to most boundary layer solutions which use analytical transformations, a general transformation for arbitrary grids is used in addition to the above transformation. Arbitrary grids are generated numerically by using a new technique of parabolic grid generation,[23] by using analytical transformations for similar solutions, or by using a combination of techniques. This approach is more flexible, and is also applicable to more general solutions of the Navier-Stokes equations. A general transformation for arbitrary grids in x-Y space to ξ-η space (corresponding to a square grid of unit step size in a rectangular domain) is then applied to Eqs.(1) using the chain rule. One metric(x_η), corresponding to normal coordinate lines, must be zero to be consistent with traditional boundary layer assumptions. The resulting equations are given by

$$(R^m v) = (Y_\xi (R^m u)_\eta - Y_\eta (R^m u)_\xi)/x_\xi \tag{3a}$$

$$u_t + uu_\xi/x_\xi + (V - Y_\xi u/x_\xi)u_\eta/Y_\eta = -p_\xi/x_\xi + [\rho(\mu+\mu_T)u_\eta/Y_\eta]_\eta/(Y_\eta Re) \tag{3b}$$

$$H_t + uH_\xi/x_\xi + (V - Y_\xi u/x_\xi)H_\eta/Y_\eta = [\rho(\mu/Pr+\mu_T/Pr_T)H_\eta/Y_\eta]_\eta/(Y_\eta Re) + p_t/\rho + (\rho[\mu(Pr-1)/Pr+\mu_T(Pr_T-1)/Pr_T](\tfrac{1}{2}u^2)_\eta/Y_\eta)_\eta/(Y_\eta Re) \tag{3c}$$

in a form convenient for computational solution.

Finite Difference Solution

The upwind difference solution which was developed is different from usual approaches primarily in three ways. First, upwind differences using either a three-point forward or backward dif-

ference (depending on the signs of appropriate eigenvalues of diagonal matrices) are used. This was suggested for the boundary layer equations,[24] but is analogous to the approach used by Hodge, Stone, and Miller previously in the solution of the incompressible Navier-Stokes equations.[25] Second, the metrics of the transformation are calculated in numerous ways. Third, the difference solution is simplified because of the upwind differences.

Upwind differences, instead of traditional central differences, are used for the nonlinear convective terms in Eqs. (3b, 3c) because of several advantages. Linearized matrix equations are more diagonally dominant when upwind differences are used, and are unconditionally stable for Eqs. (3b, 3c). Artificial viscosity is not necessary since the truncation error is diffusive, as opposed to dispersive for central differences. The magnitude of the truncation error term for an upwind difference is larger by a factor of two, but is second order also as shown below.

Truncation error depends on the grid distribution, and how the metrics are calculated. If the grid is generated numerically, then the metrics are approximated by finite differences causing a metric error. For example if $V>0$, then

$$Vu_\eta = |V|[\tfrac{1}{2}(3u_j - 4u_{j-1} + u_{j-2}) + T.E.]/[\tfrac{1}{2}(Y_{j+1} - Y_{j-1}) + M.E.] \quad (4a)$$

$$M.E. = -Y_{\eta\eta\eta}/6 + \ldots \quad (4b)$$

$$T.E. = u_{\eta\eta\eta}/3 + \ldots \quad (4c)$$

where M.E. refers to "metric error" and T.E. to "truncation error". The grid distribution could be optimized so that T.E. is zero, but M.E. could be large. Another option would be to generate the grid analytically so the metrics could be calculated

exactly, but T.E. could be large for a coarse grid. A combination of options is used however, and is very useful near singularities. For example, the Y_ξ metric is calculated analytically according to similar solutions near a leading edge singularity, while downstream of the singularity the grid may be controlled numerically to minimize truncation error. Thus, metric calculation is flexible, and independent of the difference solution.

Solution of the upwind difference equations is simplified compared to central difference methods. Although matrix bandwidth increases, iterative convergence necessary for nonlinear equations is enhanced by upwind differences because of diagonal dominance. Dominance is obtained even for flows where convection dominates, since the convective terms in Eqs. (3b, 3c) are approximated by one-sided backward or forward differences depending on the sign of their coefficients which depend on the previous iteration. Dominance is further enhanced by a two-point or three-point backward difference for time derivatives. Because of diagonal dominance, a Successive-Over-Relaxation(SOR) or tri-diagonal matrix solution technique for Eqs. (3b, 3c) is sufficient. However, a quad-diagonal matrix solution technique is used.[22] Eqs. (2, 3a) are then integrated by trapezoidal rule. A few iterations are necessary for steady or unsteady solutions, and converge rapidly if wall boundary conditions are simple.

Boundary Conditions

Boundary conditions are specified or coupled with the above finite difference solution. Because of the parabolic nature of the boundary layer equations, the normal velocity is specified at

the wall and computed at the outer boundary. The physical coordinate (y) is likewise specified at the wall and then computed at the outer boundary (for external problems). An inviscid solution provides the outer edge conditions for the velocity, enthalpy, and pressure. The pressure across the boundary layer is known since the normal pressure gradient is zero from the normal momentum equation. The no slip condition is prescribed at the wall, and only the wall enthalpy is unknown.

Various conditions are used for wall enthalpy. One option is to specify the wall temperature. An isothermal wall, or a wall temperature step corresponding to the experimental data on the plate[8] and wedge,[18] are obvious choices. Specified wall temperatures followed by an adiabatic wall is another option corresponding to experimental data on the cone.[14] A radiation equilibrium condition with a resistance-capacitance analogy to simulate conduction effects is used for the insert in the wedge.[20] Algorithms for the one-dimensional, two-dimensional, or axisymmetric heat equation for the wall can be coupled to the solution, and heat flux gages eventually investigated. However, the boundary conditions were simplified to investigate the accuracy of the computational solutions and significance of mismatches.

RESULTS

The accuracy of the upwind difference algorithm is validated by comparisons with analytical solutions and other algorithms using central differences. The accuracy of the difference solutions across a thermal mismatch and the significance of mismatches are then implied by additional comparisons with experimental data.

Finally, unique results for an unsteady problem are presented. Results are computed for three simple geometric shapes to avoid additional complexities caused by curvature. These shapes include a flat plate, a cone, and a wedge.

Flat Plate

First, the skin friction was computed on a flat plate using the upwind difference algorithm, since an exact solution is available for incompressible flow. Since the algorithms are for compressible flow, a Mach number of 0.001 and constant temperature were assumed. The same 30x30 grid generated by a central difference algorithm with an analytical transformation was used. The metrics were very sensitive to how they were approximated, and therefore the Y_ξ metric was calculated analytically. The skin friction was less than the exact theoretical solution by no more than one percent, whereas the central difference algorithm had no more than a one-half percent overshoot. Thus, the accuracy for incompressible flow is validated.

Other grids were also used since difference algorithms are very grid dependent. The upwind algorithm did not diverge when a very coarse grid was used, but the central algorithm did. Both algorithms demonstrated second-order convergence when the step size decreased. Second order upwind differences were usually necessary, however, since the skin friction with first order upwind differences for the above grid was only within eight percent. Similar results were also obtained for a thermal mismatch.

Next, the upwind algorithm was validated for turbulent, incompressible flow over a plate with a thermal mismatch. The heat

transfer for the unheated/heated plate in Figure 1 with a 11°K temperature step was computed, and agrees well with experimental data as shown in Figure 4. Predictions for laminar and turbulent flow with and without the mismatch are also shown. Note that the percentage change in heat transfer due to the thermal mismatch is greater for laminar flow. The accuracy was more sensitive to turbulence modeling than to the numerics for a 61x59 grid with several grid points in the sublayer. Therefore, computational accuracy for a mismatch is addressed better using laminar data.

Cone

Since steady wall temperature data are available for both laminar and turbulent flow over a cone with a thermal mismatch,[14] upwind difference solutions were computed to validate accuracy across a mismatch. If the cooled nose of the cone is assumed to have an isothermal wall and no boundary layer/flow interaction, then the heat transfer prediction is analogous to a flat plate and wedge according to boundary layer theory, except for an increase in heat transfer by a factor of $\sqrt{2}$. Thus, the computed heat transfer coefficients at the nose can be compared with analytical solutions. Then, the computed adiabatic wall temperature distribution downstream of the mismatch is compared to the measured wall temperature distribution.

The isothermal heat transfer coefficient on the cooled nose, predicted by the upwind difference solution for compressible flow with a fine grid (61x59), compared with the central difference solution to the third decimal. The magnitude of the heat transfer coefficient also compared within a few percent to approximate

analytical solutions depending on the viscosity law. Further comparisons are not necessary since Reynold's analogy leads back to the skin friction comparisons above for incompressible flow over a flat plate, if the viscosity is assumed constant.

Next, adiabatic wall temperatures downstream of the thermal mismatch were computed and compared. Durgin obtained excellent comparisons between the data and approximate analytical solutions,[14] if actual wall temperatures were used upstream of the mismatch. The measured and predicted wall temperature distributions along the surface of the cone are shown in Figure 5 for both laminar and turbulent flow. Good agreement is shown considering that a uniform temperature was assumed on the cooled nose. In fact, this illustrates that the error is no greater than the experimental error in maintaining an isothermal wall on the nose.

If the analytical and computational solutions are amplified just downstream of the thermal mismatch and discontinuity, however, a discrepancy is evident. The jump in heat transfer or wall temperature at the mismatch is smeared by numerical truncation error, and is smeared by conduction effects in any experiment. Therefore, the required grid size at the mismatch depends on the material properties. To account for these properties, and to also compute wall temperatures in general, the computational solution may need to be coupled with a computational solution of the heat equation for the materials. Since the wall temperatures are usually transient, the unsteady equations are solved.

Wedge

Several algorithms were used to predict the heat transfer on

the wedge shown in Figure 3 with a thermal mismatch. Approximate analytical solutions, central difference solutions of the steady boundary layer equations, solutions of the Navier-Stokes equations using an explicit MacCormack's algorithm, upwind difference solutions of the steady boundary layer equations, and upwind difference solutions of the unsteady boundary layer equations have been compared to limited experimental data on the wedge for constant deflection angle and for a pitch manuever. Steady results for a thermal mismatch corresponding to this data have been obtained by assuming an appropriate wall temperature step. The analytical solutions and steady boundary layer results are given first. Since the flow was hypersonic and some viscous-shock interaction was expected, solutions of the Navier-Stokes equations are then presented. Finally, since transient effects have been postulated, upwind difference solutions of the unsteady boundary layer equations coupled with a wall condition for a thermal mismatch are presented for a pitching wedge.

Several steady solutions of the boundary layer equations for the wedge with a specified wall temperature step of 95°K were computed. At 14° deflection angle, the ratio of the heat transfer coefficient to a reference coefficient at 0° is shown in Figure 6. Computational and approximate analytical solutions compare as mentioned above for laminar flow on a cone. Although predictions account for most of the significant decrease in heat transfer coefficient, the experimental heat transfer is lower near the thermal mismatch, but recovers and agrees downstream.

Since a strong viscous-shock interaction is possible at hyper-

sonic speeds over the front one-third of the wedge (especially at a lower deflection angle of three degrees), the two-dimensional Navier-Stokes equations were solved computationally by Roberts using a 62x30 exponentially stretched grid.[24] Results for both an isothermal wall and a thermal mismatch with an assumed temperature step of 88° K are shown in Figures 7 and 8. The ratio of the wall pressure to freestream pressure is compared in Figure 8 to the inviscid solution, which is used by boundary layer theory. The wall pressure is higher, as expected because of viscous-shock interaction. The thickening of the thermal layer downstream of the thermal mismatch then caused another interaction, which is shown by a small increase in wall pressure further downstream. However, the interactions only cause small increases in the heat transfer as shown in Figure 8. The heat transfer prediction is also higher than the experimental data.

Since time variations in heat transfer coefficient have been postulated, unsteady effects and solutions were investigated. Numerous effects, although perhaps small, cause time variations in the wind tunnel. Among these are variations in tunnel conditions, increasing wall temperatures near the leading edge, conduction, and radiation. An advantage of computational methods is that these effects can be investigated separately. Therefore, the radiation equilibrium boundary condition with the resistance-capacitance analogy was used downstream of the stainless steel/FRSI interface to simulate thermal lag due to conduction. Since the flow is hypersonic, a quasi-steady approach (steady inviscid solutions) is used for edge conditions, and pitch rate effects

neglected. The unsteady boundary layer equations were then coupled with wall boundary conditions, and solved for a simulated injection and pitch manuever of the wedge in the wind tunnel.

The wall temperature distribution was thus obtained downstream of the thermal mismatch at each time step. After injection to a constant 14° deflection angle, the wall temperatures were allowed to reach equilibrium. The wall temperature distribution at equilibrium is shown in Figure 9 corresponding to the highest temperatures. These temperatures also correspond to the start of the pitch manuever. After the pitch down to 3°, the wall temperatures decrease, but lag the lowest wall temperatures shown which occur after the five second hold at 3° (and before the pitch up to 14°). At the end of the pitch manuever, the wall temperatures are less than the equilibrium temperatures due to the lag. Equilibrium is eventually reached again with the radiative heat rate equal to the convective heat rate.

The convective heat rate distribution was also computed at each time step, but the postulated hysteresis loop is best illustrated at a given location as shown in Figure 10. The heat transfer coefficients at 14° (and start of the pitch manuever) decrease as the wedge is pitched down. During the five second hold at 3°, the heat transfer increases. Then as the wedge is pitched up, the heat transfer is higher than during the pitch down, and increases to a maximum at the end of the pitch manuever. As the wall temperatures increase towards equilibrium, the heat transfer eventually decreases back to equilibrium. It should be noted that this significant time variation in heat transfer occurs just

downstream of a thermal mismatch. Further downstream, the variation and hysteresis loop are smaller. However, unsteady flow effects were very small.

Although the external flow was assumed to be quasi-steady, unsteady terms were still included in the boundary layer. Some additional lag in the wall temperatures and an overshoot in heat transfer could be caused due to finite convection velocities near the wall. Solutions with and without the unsteady terms were computed, and temporal truncation error was checked by using smaller time steps. A very small overshoot in the heat transfer ratio of less than one-tenth percent was obtained when a very small time step of 25 milliseconds was used. Such a small effect is expected for hypersonic flow where only a very small fraction of the boundary layer is subsonic. The time scale for the hypersonic flow is essentially three or more orders of magnitude less than the time scale for heat conduction at the wall. Thus, a completely quasi-steady approach using steady boundary layer solutions or approximate analytical solutions would be accurate. For lower velocities and higher pitch rates, unsteady solutions may be required.

CONCLUSIONS AND RECOMMENDATIONS

The flexibility of algorithms using upwind differences and a general transformation has been demonstrated due to improved diagonal dominance. Steady, unsteady, and quasi-steady solutions were computed efficiently, and wall boundary conditions with dramatically different time scales were coupled with the solution. Although alternative solutions are available for a boundary

layer, the unsteady nature of viscous solutions of the Navier-Stokes equations may necessitate a similar approach. This flexible approach is also applicable to Navier-Stokes solutions.

The accuracy of an upwind algorithm for the unsteady boundary layer equations was also validated by comparisons with analytical solutions, central difference solutions, and experimental data. The error in skin friction and heat transfer was shown to be larger for upwind differences than for central differences, but of the same order magnitude. Explicit artificial viscosity, which often degrades the accuracy of central difference solutions, was not neccessary with upwind differences even for very coarse grids. However, second-order upwind differences were necessary with coarse grids, especially for mismatches.

The accuracy of difference methods across a thermal mismatch, and significance of mismatches, was also demonstrated. Second-order solutions, but not first-order, were shown to be accurate across a mismatch. The solutions and the experimental data also demonstrated that the heat transfer can be significantly affected locally by mismatches. The dependence on thermal properties and wall boundary conditions were demonstrated by predicting time variations in the heat transfer during a pitch manuever of a wedge with a thermal mismatch.

Since modern vehicles and heat flux instrumentation have numerous material interfaces where thermal and chemical mismatches are possible, some method should be used to evaluate the significance of the mismatch. Analytical approximations can often be used, and appropriate wall boundary conditions should be coupled with

second-order implicit finite difference solutions.

REFERENCES

1. Chung, P. M., Liu, S. W., and Mirels, W., "Effect of Discontinuity of Surface Catalycity on Boundary Layer Flow of Dissociated Gas," Int. J. Heat Mass Transfer, Vol. 6, 1963, pp. 193-210.

2. Sheldahl, R. E. and Winkler, E. L., "Effect of Discontinuities in Surface Catalytic Activity on Laminar Heat Transfer in Arc-Heated Nitrogen Streams," NASA TN D-3615, 1966.

3. Stewart, D. A., Rakich, J. V., and Lanfranco, M. J., "Catalytic Surface Effects Experiment on Space Shuttle," AIAA-81-1143, 1981.

4. Rakich, J. V., Stewart, D. A., and Lanfranco, M. J., "Results of a Flight Experiment on the Catalytic Efficiency of the Space Shuttle Heat Shield," AIAA-82-0944, 1982.

5. Scott, C. D. and Derry, S. M., "Catalytic Recombination and The Space Shuttle Heating," AIAA-82-0841, 1982.

6. Curry, D. M., Rochelle, W. C., Chao, D. C., Ting, P. C., "Space Shuttle Orbiter Nose Cap Thermal Analysis," AIAA-86-0388, 1986.

7. Scesa, S., "Experimental Investigation of Convection Heat Transfer to Air From a Flat Plate with a Stepwise Discontinuous Surface Temperature," M. S. Thesis, U. Calif. Berkeley, CA, 1949.

8. Reynolds, W. C., Kays, W. M., and Klein, S. J., "Heat Transfer in the Turbulent Incompressible Boundary Layer, Part II-Step Wall Temperature Distribution," NASA Memo. 12-2-58W, 1958.

9. Ede, A. J. and Saunders, O. A., "Heat Transfer From a Flat

Surface to a Parallel Stream of Water." Proc. Instit. Mech. Eng., Vol. 172, 1958, pp. 743-756.

10. McCroskey, W. J., "Effect of a Stepwise Distribution of Heat Transfer on the Supersonic Flow Over a Flat Plate," ICEA Tech. Note 13, 1963.

11. McCroskey, W. J., "The Effect of a Stepwise Distribution of Heat Transfer on the Compressible Flow Over a Flat Plate." Int. J. Heat Mass Transfer, Vol. 9, 1966, pp. 593-595.

12. Praharaj, S. C. and Foster, L. D., "Orbital Flight Test Shuttle External Tank Flowfield and Aerothermal Analysis," AIAA-84-1750, 1984.

13. Durgin, F. H., "An Insulating Boundary-Layer Experiment." J. Aerospace Sciences, Vol. 26, 1959, pp.450-451.

14. Durgin, F. H., "An Experiment on the Insulating Properties of Boundary-Layers," Aero. Eng. Thesis, Mass. Inst. Tech., Cambridge, Mass., 1957.

15. Hodge, J. K., Woo, Y. K., and Cappelano, P. T., "Parameter Estimation for Imbedded Thermocouples in Space Shuttle Wind Tunnel Test Articles with a Nonisothermal Wall," AIAA-83-1533, 1983.

16. Woo, Y. K., "Transient Heat Transfer Measurement Technique in Wind Tunnel and Data Analysis Technique Using System Identification Theory," Aero. Eng. M. S. Thesis, Air Force Inst. Tech., Wright-Patterson AFB, OH, 1982.

17. Hodge, J. K., Chen, A. J., and Hayes, J. R., "Unsteady Heat Transfer Coefficient Estimation for Long Duration," AIAA-86-1240, 1986.

18. Cebeci, T. and Smith, A. M. O., Analysis of Turbulent

Boundary Layers, Academic Press, New York, 1974, Chap. 6.

19. Kim, J. S. and Chang, K. S., "Calculation of Incompressible and Compressible Unsteady Boundary Layers by a Noniterative Finite Difference Method," AIAA-84-1639, 1984.

20. Lange, K. J., "Unsteady Solution of the Boundary Layer Equations with Application to Space Shuttle Tiles," Aero. Eng. M. S. Thesis, Air Force Inst. Tech., Wright-Patterson AFB, OH, 1984.

21. Coffey, D. E. Jr., "Adaptive-Grid Optimization for Minimizing Steady-State, Truncation Error," Astro. Eng. M. S. Thesis, Air Force Inst. Tech., Wright-Patterson AFB, OH, 1985.

22. Chen, A. J., "Numerical Solution of Laminar and Turbulent Boundary Layer Equations Including Transition, and Experimental Study of a Flat Plate with a Blunt Fin at Incidence," Aero. Eng. M. S. Thesis, Air Force Inst. Tech., Wright-Patt. AFB, OH, 1986.

23. Hodge, J. K., Leone, S. A., and McCarty, R. L., "Non-Iterative Parabolic Grid Generation for Parabolized Equations," AIAA-85-1528-CP, 1985.

24. Anderson, D. A., Tannehill, J. C., and Pletcher, R. H., Computational Fluid Mechanics and Heat Transfer, McGraw-Hill, New York, 1984, pp.344-346.

25. Hodge, J. K., Stone, A. L., and Miller, T. E., "Numerical Solution for Airfoils Near Stall in Optimized Boundary-Fitted Curvilinear Coordinates," AIAA J., Vol. 17, 1979, pp. 458-464.

26. Roberts, T. K., "Numerical Solution of a Nonisothermal Wall Using the Two-Dimensional Navier-Stokes Equations," Aero. Eng. M. S. Thesis, Air Force Inst. Tech., Wright-Patt. AFB, OH, 1985.

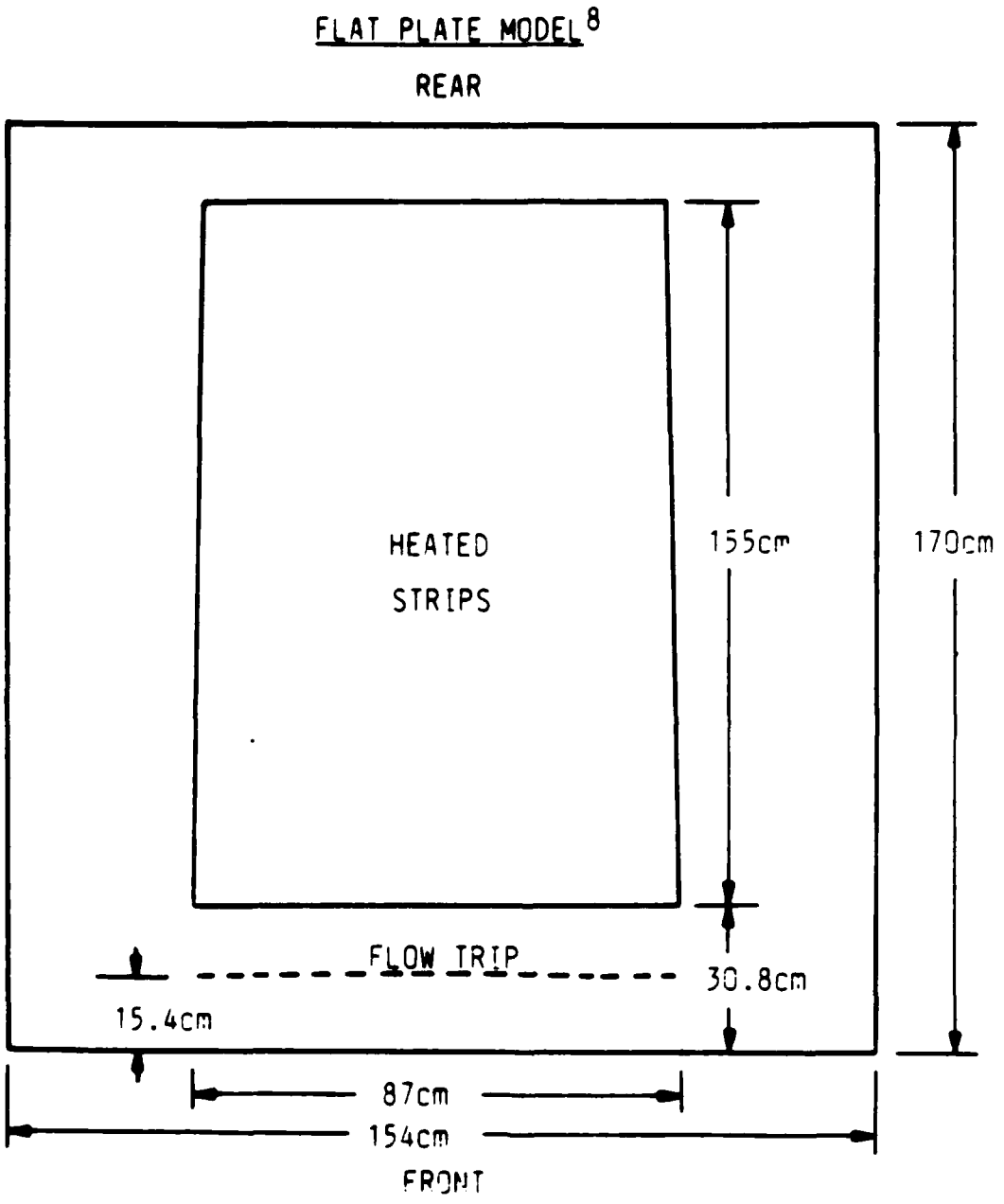

Figure 1. Flat Plate Model With Unheated Heated Wall

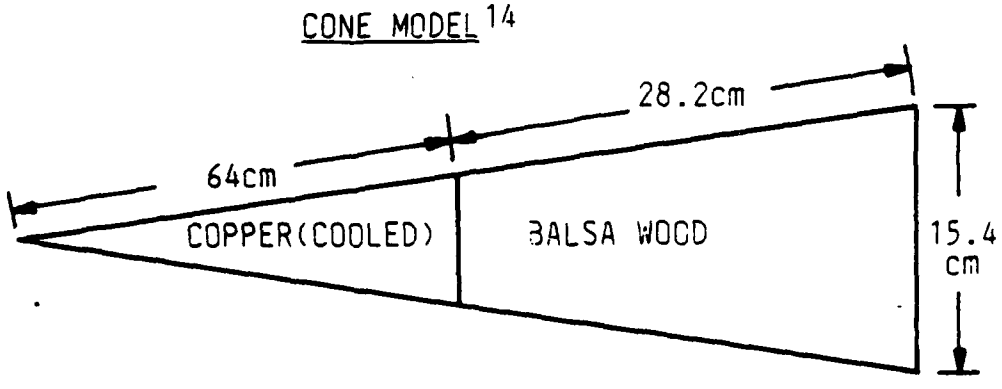

Figure 2. Axisymmetric Cone Model With Cooled/Adiabatic Wall

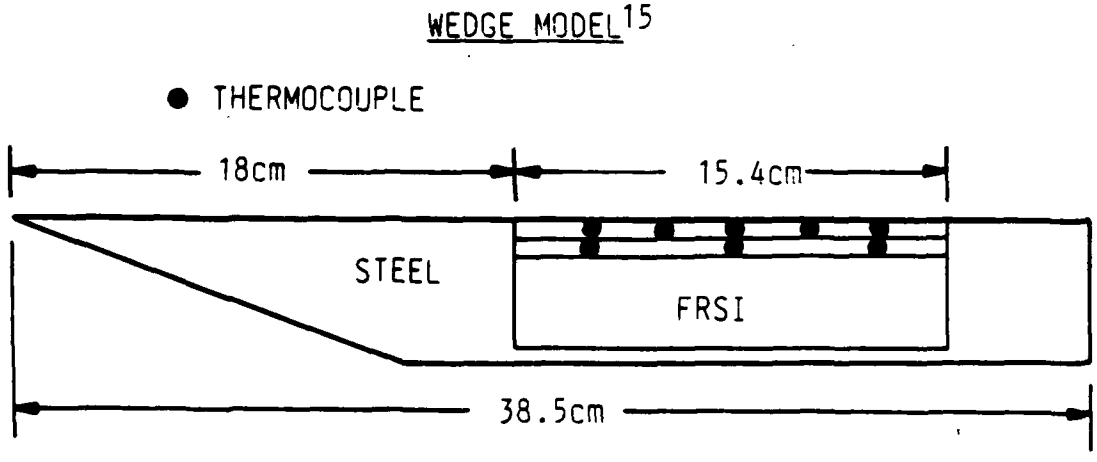

Figure 3. Wedge Model With Steel/FRSI Interface

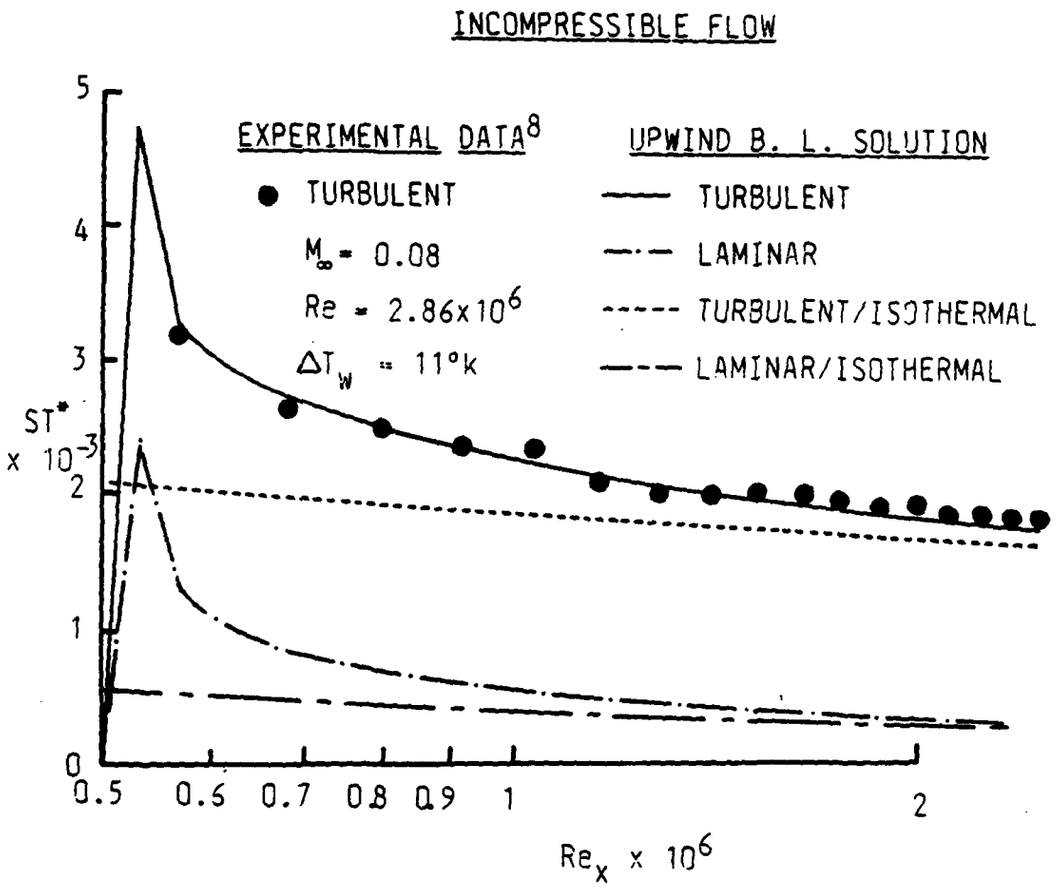

Figure 4. Stanton Number Comparison for Turbulent, Incompressible Flow Over Plate With Thermal Mismatch

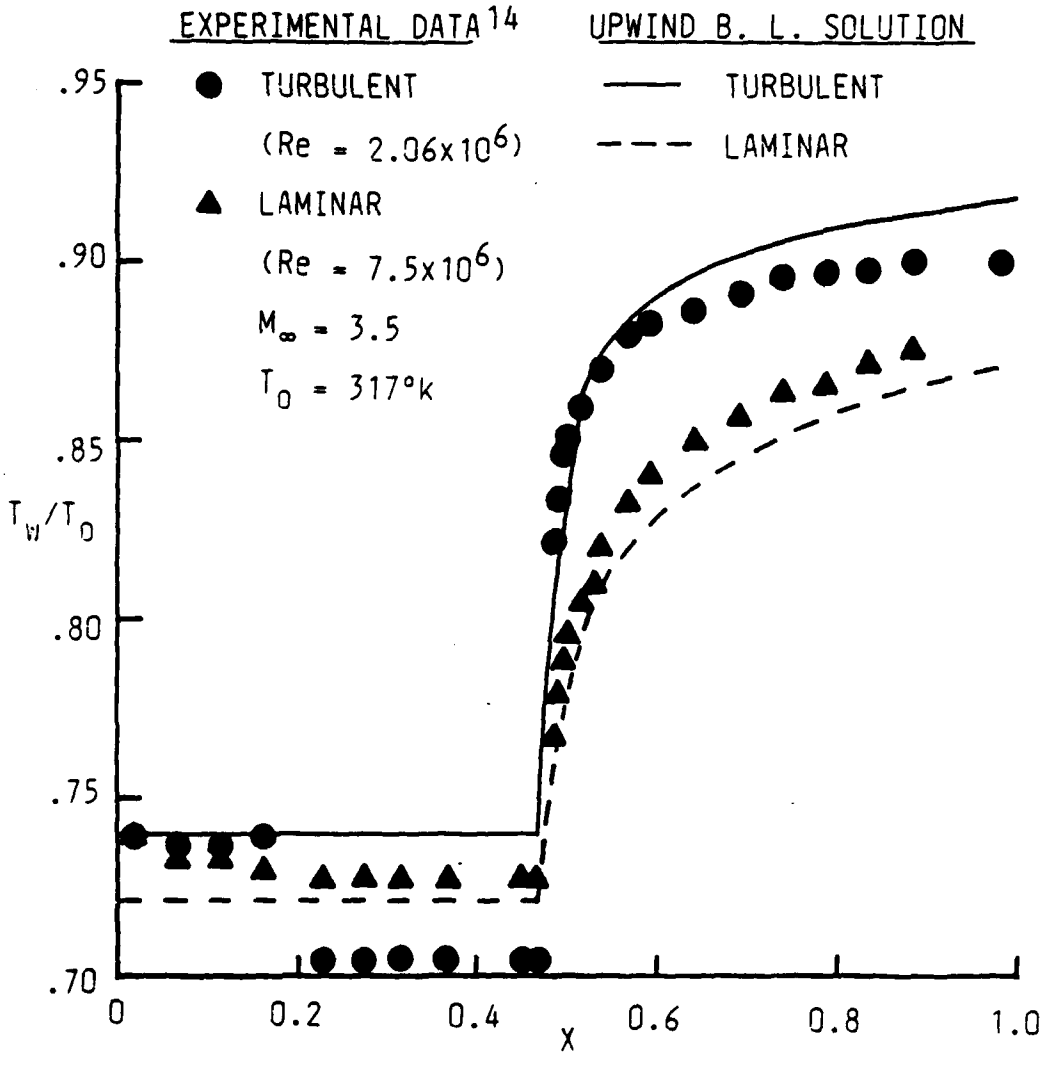

Figure 5. Wall Temperature Comparison for Laminar and Turbulent Flow Over Cone With Thermal Mismatch

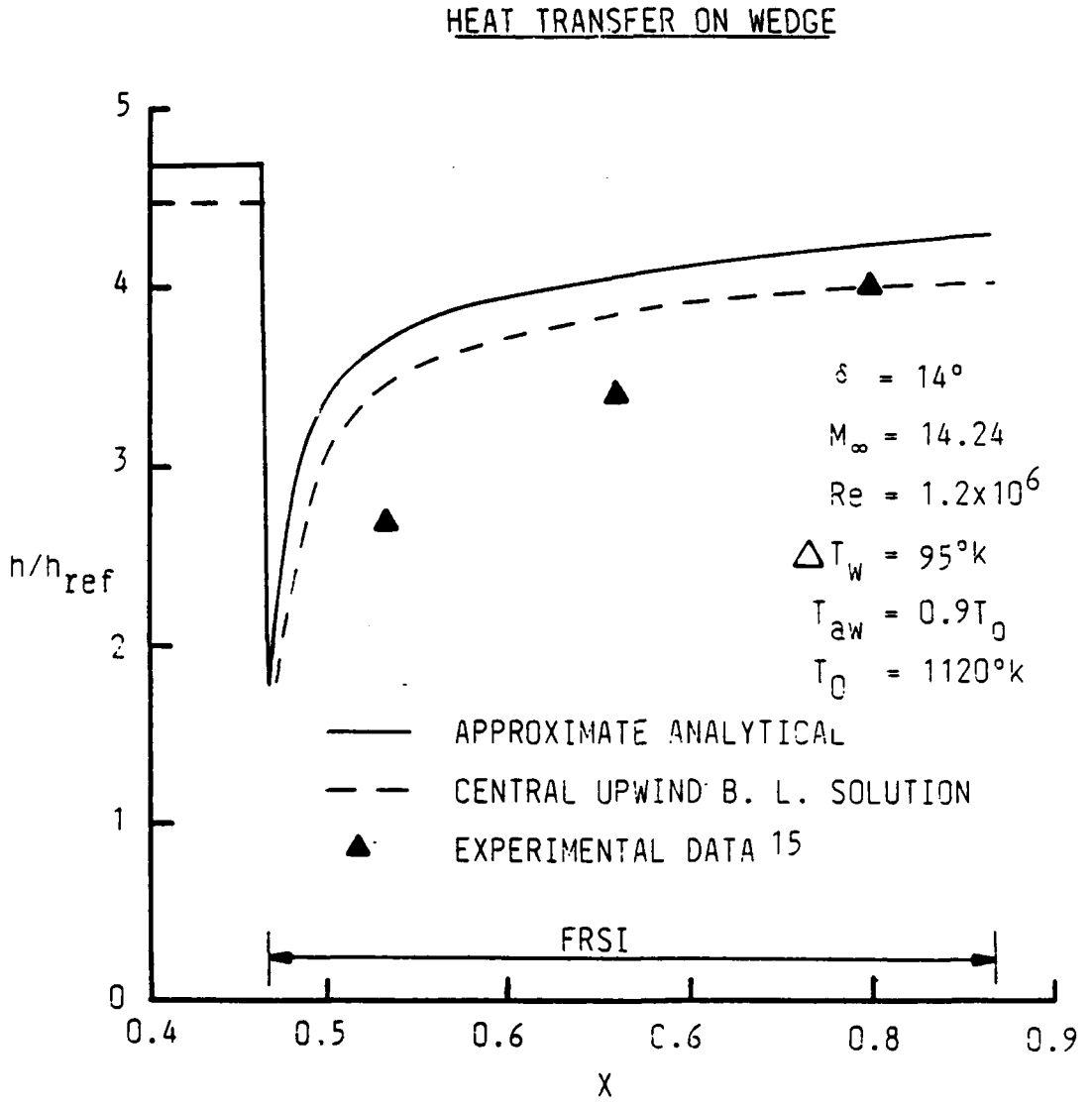

Figure 6. Steady Heat Transfer Coefficient for Laminar Flow Over Wedge With Thermal Mismatch

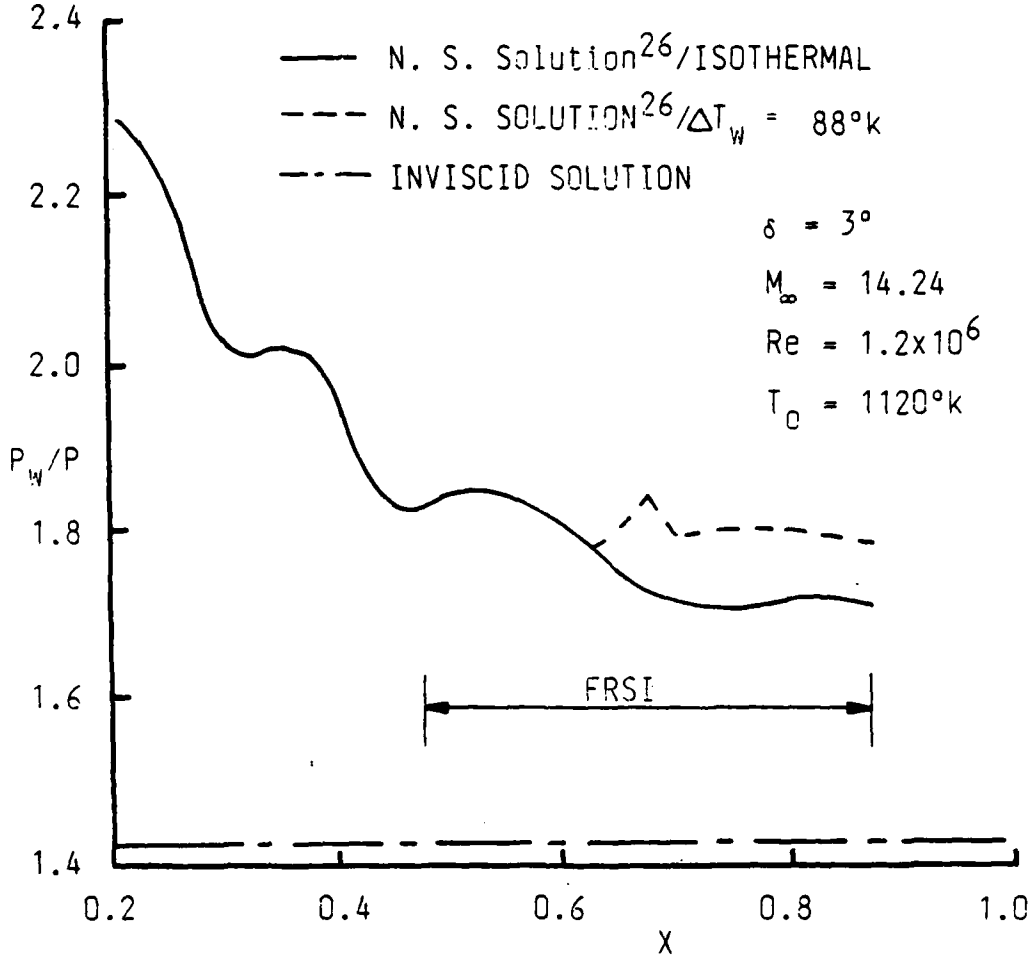

Figure 7. Pressure on Wedge from Navier-Stokes Solution With and Without Thermal Mismatch

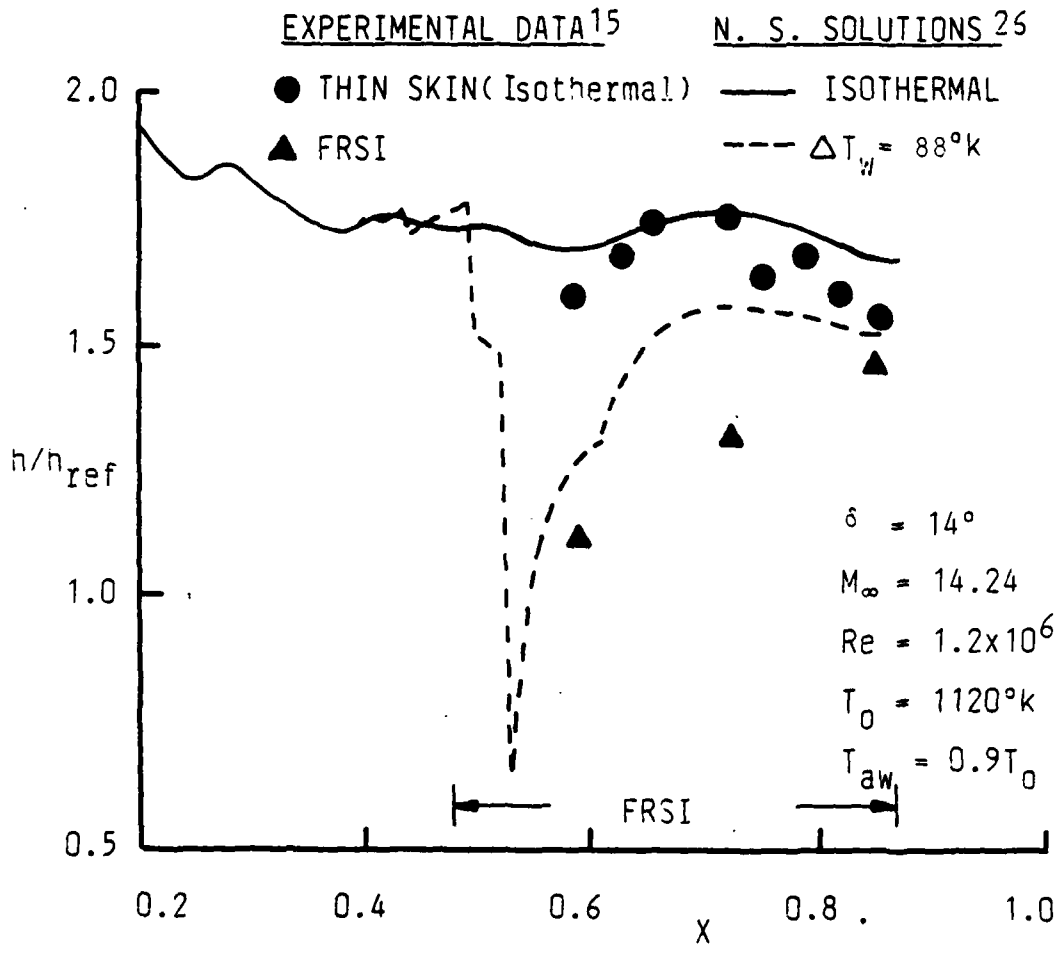

Figure 8. Heat Transfer Coefficient on Wedge from Navier-Stokes Solution With and Without Thermal Mismatch

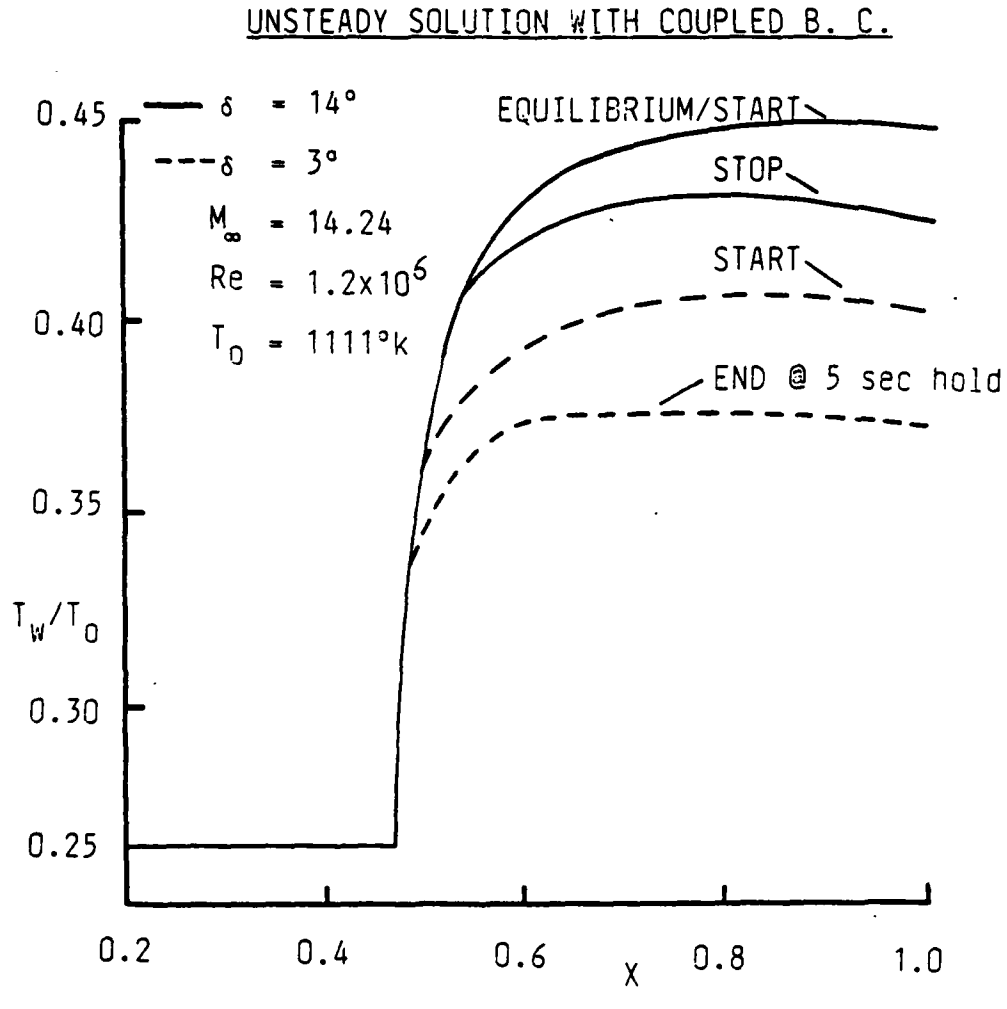

Figure 9. Transient Wall Temperature Distribution on Wedge During Pitch Manuever

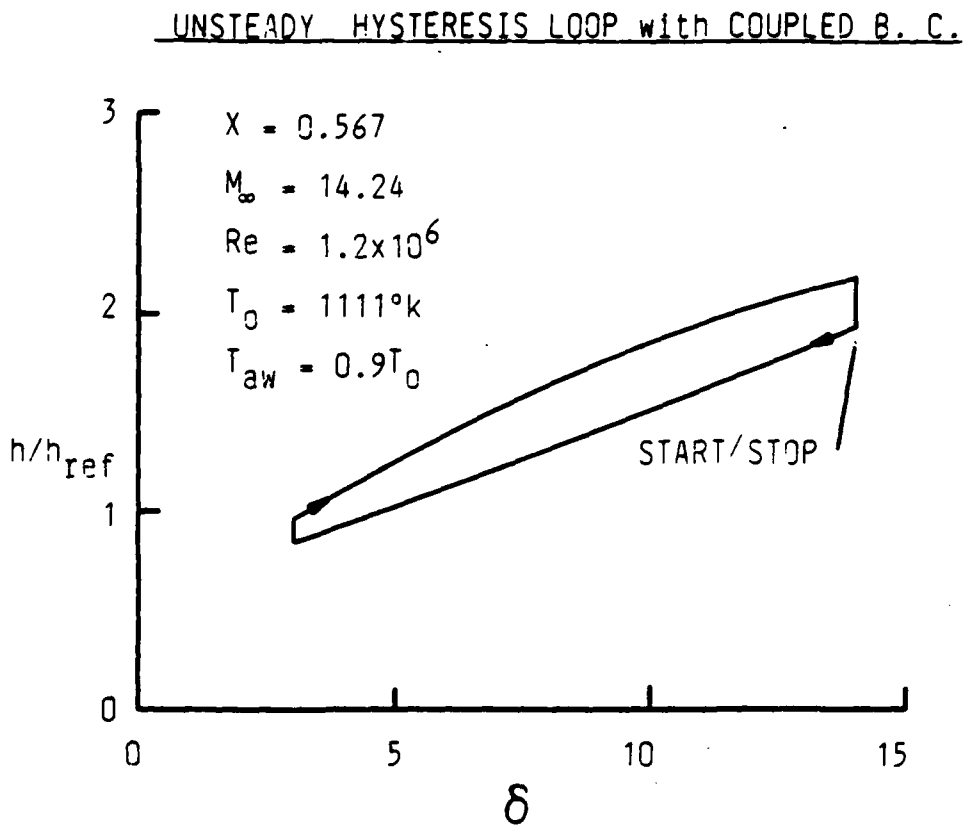

Figure 10. Transient Heat Transfer Coefficient on Wedge During Pitch Manuever Showing Hysteresis Loop